Bipyridine-based conjugated microporous polymers for boosted photocatalytic U(VI) separation

Yun Xie[a], Zifan Li[a], Chenchen Liu[b], Qiming Song[b], Yunhai Liu[a], Zhibin Zhang*[a], and Bin Han*[b]

[a] State Key Laboratory of Nuclear Resources and Environment, East China University of Technology, Nanchang, Jiangxi 330013, P.R. China

[b] Guangdong Basic Research Center of Excellence for Ecological Security and Green Development, Key Laboratory for City Cluster Environmental Safety and Green Development of the Ministry of Education, School of Ecology, Environment and Resources, Guangdong University of Technology, Guangzhou, 510006, P. R. China

*Corresponding Authors: E-mail: zhbzhang@ecut.edu.cn (Z. B. Zhang); hanbin@gdut.edu.cn (B. Han)

Experimental section

Text S1 Chemicals and materials

All reagents used in the experiment are analytically pure and no further purification is required. 3,6-dibromocarbazole, 1,4-Benzenediboronic acid bis(pinacol) ester, 4,4'-Dibromobiphenyl, and 5,5'-Dibromo-2,2'-bipyridine were purchased from Jilin Chinese Academy of Sciences-Yanshen Technology Co., Ltd. Other chemicals (analytical reagent class) were provided by Adamas-beta. Ultrapure water (18 MΩ·cm) was used in all experiments.

Text S2 Synthesis of 3,3',6,6'-Tetrabromo-9,9'-bicarbazole (Cz-4Br)

The donor molecule 3,3',6,6'-Tetrabromo-9,9'-bicarbazole was synthesized following procedures outlined in prior studies[1], with certain modifications. Specifically, a solution containing potassium permanganate (2.92 g) and 3,6-dibromocarbazole (2.00 g) in 40 ml of acetone was stirred for 5 hours at 333 K. The residue was extracted with CH_2Cl_2 (150 ml). Following this, the compound was isolated via spin distillation and subsequently washed with methanol multiple times to yield a white solid (1.24 g, 62%).

Text S3 Synthesis of CMPs

Cz-4Br (97.2 mg, 0.15 mmol), 1,4-Benzenediboronic acid bis(pinacol) ester (148.5 mg, 0.45 mmol), 4,4'-Dibromobiphenyl (46.8 mg, 0.15 mmol), and Pd $(PPh_3)_4$ (20 mg), 20 ml N, N-Dimethylformamide (DMF) were added to a 100 ml Shrek tube, and freeze-pump-defrost three times. Then a K_2CO_3 solution (2.0 M, 5 ml) was added to the above mixture. Reaction tubes were heated at 150 ℃ for 48 hours. End of the reaction, the reaction tube was cooled to room temperature and washed with methanol and dichloromethane sequentially until the effluent was clear and transparent. Put into a vacuum drying oven and dry at 50 ℃ for 24 hours, product Cz-Bph was obtained. The Cz-Bpy was synthesized similarly to Cz-Bph by replacing 4,4'-Dibromobipyridine with 5,5'-Dibromo-2,2'-bipyridine (47.1 mg, 0.15 mmol). The element content of Cz-Bph: C: 85.73; H: 7.14; N: 4.74. The element content of Cz-Bpy: C: 82.39; H: 6.46; N: 7.86.

Text S4 Photocatalytic experiments

The U(VI) separation experiments were conducted in a 100 mL quartz sandwich reactor cooled with circulating water at the temperature of 20 ℃. Specifically, 5 mg of CMPs was mixed with 25 mL uranium solution. The pH of the uranium solution was adjusted by 0.01 mol/L $NaOH/HNO_3$. The mixture was stirred in the dark for 60 min before being illuminated with a 300 W Xenon lamp ($\lambda \geq 420$ nm). A 0.45 μm membrane was used to filter the solution after a specific time. The concentration of UO_2^{2+} was confirmed by using a UV-vis spectrophotometer and (Inductively Coupled Plasma Optical Emission Spectrometer) ICP-OES[2–5]. The removal rate of U(VI) can be calculated as C_t/C_0, that C_0 and C_t are the initial concentrations of U(VI) and the concentrations at a time (t). All tests were taken three times and averaged. The error bars in the figures represent the standard deviations from triplicate tests.

Text S5 Characterization methods

The crystalline phase, morphology, and chemical state of elements of samples were characterized by X-ray diffraction (XRD, Bruker D8 Advance), scanning electron microscopy (SEM, FEI Nova Nano SEM 450), Fourier-transform infrared (FT-IR, Bruker Tensor II) spectra, and X-ray photoelectron spectroscopy (XPS, AXIS Supra+). Shimadzu UV-3101PC spectrophotometer was used to obtain ultraviolet-visible (UV-visible) absorption spectra. All of the electrochemical experiments were tested in 0.2 M sodium sulfate solution (pH=7.0) through a three-electrode electrochemical workstation (Parstat 4000A, Ametek). The working electrode consists of an ITO glass plate coated with a photocatalyst slurry. Specifically, 1 mg of catalyst, 1 mL of ethanol, and 20 μL of Nafion D-520 were combined and subjected to 30 minutes of ultrasound treatment. Subsequently, 200 μL of the slurry was evenly deposited onto the 1 × 1 cm^2 ITO glass plate and allowed to dry in air. The counter electrode is platinum foil, and a saturated Ag/AgCl electrode serves as the reference electrode. The temperature-dependent photoluminescence spectra (TD-PL) were explored on the Shimadzu RF-6000 spectrometer with the assistance of a liquid nitrogen thermostat (LNT,

JouleYacht, China). The elemental contents of the as-prepared photocatalysts were verified using an elemental analyzer (Elementar Vario Micro Cube).

Text S6 Computational details

The structure of CMPs and adsorption structures of $[U(VI)O_2(H_2O)_2]$@Cz-Bpy were optimized at the PBE0/DEF2-SVP+SDD level using the Gaussian 16 software. For all the calculations, the dispersion force contributed to energy is considered using the Grimme D3[6] method, and the solvent effect was described by the conductor-like polarizable continuum model (C-PCM).[7] The electron/hole distributions and Sr/Sm index were obtained with Multiwfn and Vesta[8,9].

Text S7 Comparison of photocatalytic activity

We employed the following equation to assess the photocatalytic performance[10,11].

$$R = \frac{1000XCV}{238MT}$$

where R is the kinetic photoreaction rate, μmol/(g·h); X is the removal efficiency caused by irradiation (X=0~100%); C is the concentration of U(VI), mg/L; V is the volume of solution, mL; M is the mass of photocatalysts, mg; and the T is the irradiation time, h. The 1000 is a constant and the 238 is the molecular weight of uranium.

Text S8 Stability and reusability.

After each photocatalytic reaction, the used materials were isolated from the solution through filtration. Subsequently, the filter membrane was immersed in a 50 mL 0.2 mol L^{-1} Na_2CO_3 solution, subjected to sonication for 5 minutes to disperse the solid material in the solution, and then stirred for 6 hours. Following this, the photocatalyst was separated from the uranium solution by filtration, washed, and dried for subsequent reuse. The filtrate was recycled for subsequent elution cycles, enabling the concentration of uranyl carbonate solution to increase progressively, thereby achieving the recovery and enrichment of uranyl ions.

Text S9 H_2O_2 production test and detection of H_2O_2.

The photochemical synthesis of H_2O_2 was performed in a 50 mL glass tube, which included 5 mg of photocatalyst and 25 mL of deionized water, maintained at a temperature of 25 ºC under atmospheric conditions. The suspension was then subjected

to ultrasonication for approximately 3 minutes to ensure even dispersion of the photocatalyst. Next, the suspension was oxygenated for 20 minutes. Subsequently, the reaction mixture was illuminated/ultrasonicated using a 300 W xenon lamp source ($\lambda >$ 420 nm). The method of detecting H_2O_2, 0.5 mL of $C_8H_5KO_4$ aqueous solution (0.2 M), and 0.5 mL of KI aqueous solution (0.8 M) was added into 1 mL of reaction liquid and then kept for 60 min. The concentration of H_2O_2 was calculated at 350 nm and detected by a UV-vis spectrophotometer.

Text S10 Coumarin experiment.

To quantify the •OH radicals generated during the photoreaction, 5 mg of photocatalyst was dispersed in 25 mL of a 1 mmol/L coumarin aqueous solution. After irradiation for a specified duration, 1.0 mL of the solution was extracted. The concentration of 7-hydroxycoumarin was analyzed via photoluminescence (PL) with an excitation wavelength of 345 nm.[12]

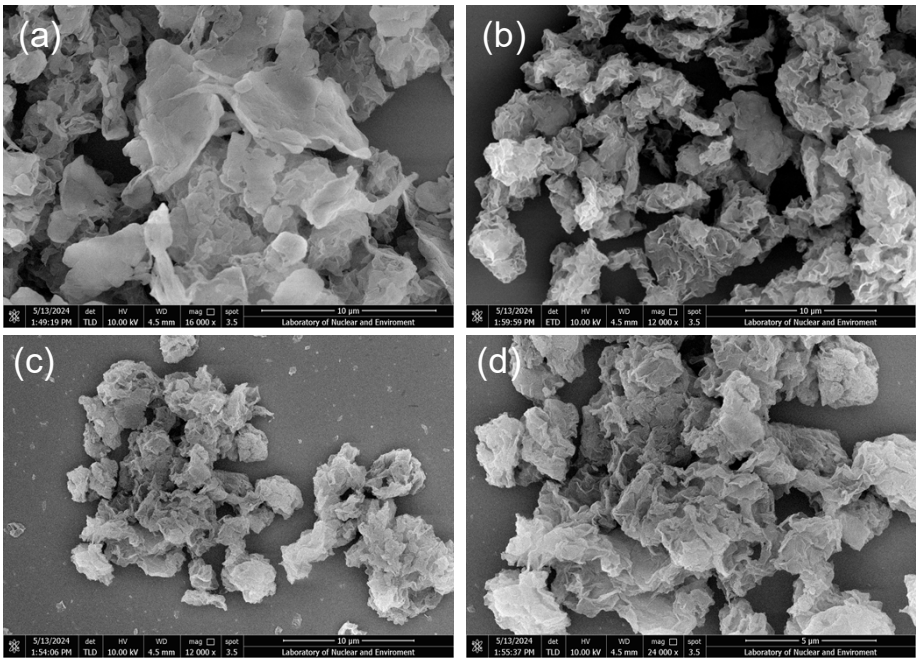

Fig. S1. SEM of (a,b) Cz-Bph and (c,d) Cz-Bpy.

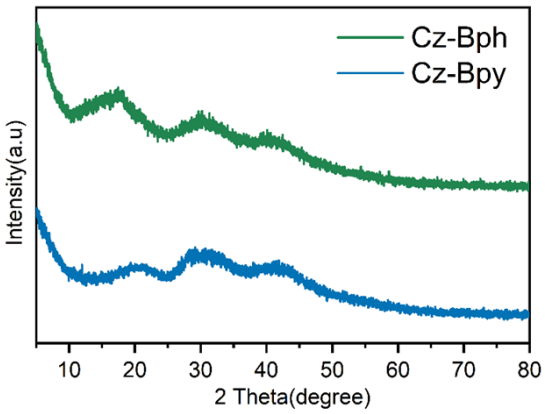

Fig. S2. The XRD of Cz-Bph and Cz-Bpy.

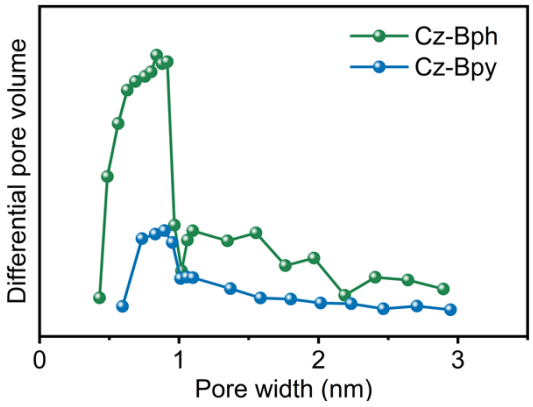

Fig. S3. The corresponding pore diameters of Cz-Bph and Cz-Bpy.

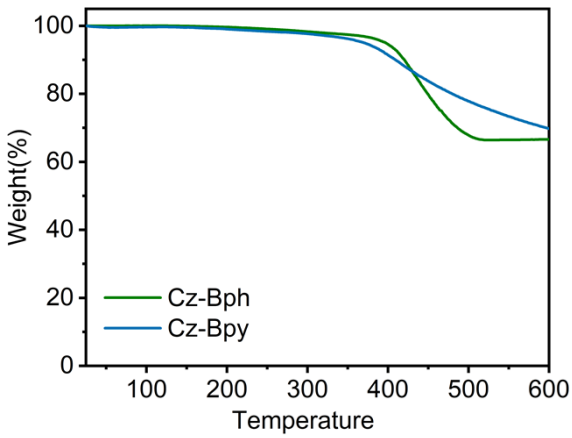

Fig. S4. The thermogravimetric analysis of Cz-Bph and Cz-Bpy.

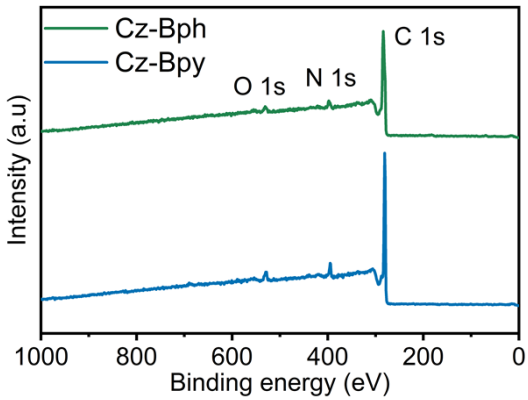

Fig.S5. The XRD of Cz-Bph and Cz-Bpy.

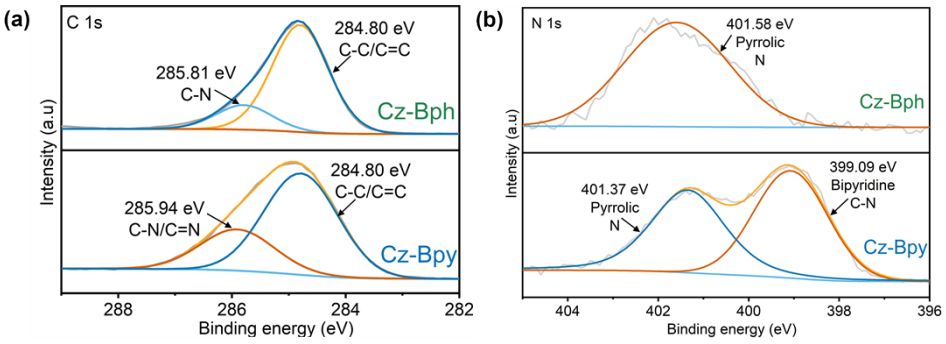

Fig. S6. XPS spectra of Cz-Bph and Cz-Bpy (a) C 1s spectra and (b) N 1s spectra.

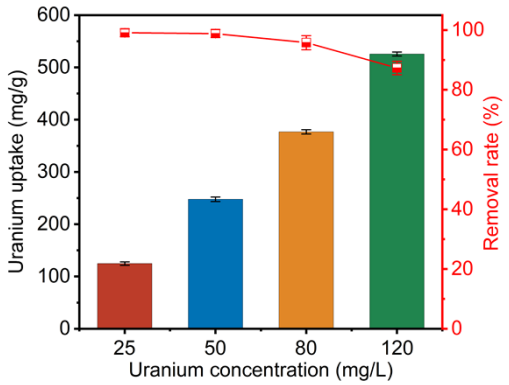

Fig. S7 Influence of various U(VI) concentration (condition: Cz-Bpy as photocatalyst, pH = 5.0, m/V = 0.2 g/L, and T = 293 K). The error bars in the figure represent the standard deviations from triplicate tests.

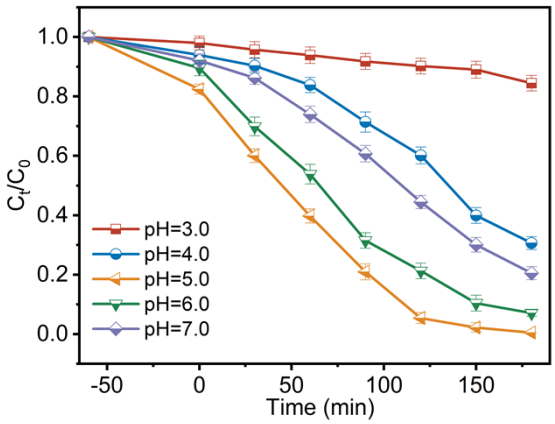

Fig. S8 The separation of U(VI) by Cz-Bpy on various pH value (C_0 = 50 mg/L, m/V = 0.2 g/L, and T = 293 K). The error bars in the figure represent the standard deviations from triplicate tests.

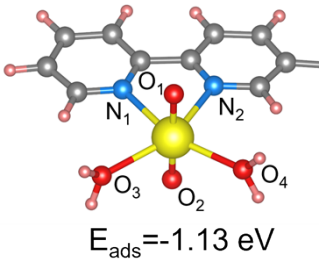

Fig. S9. The adsorption model and energy for the U(VI)O_2(H_2O)$_2$ adsorbed onto Cz-Bpy.

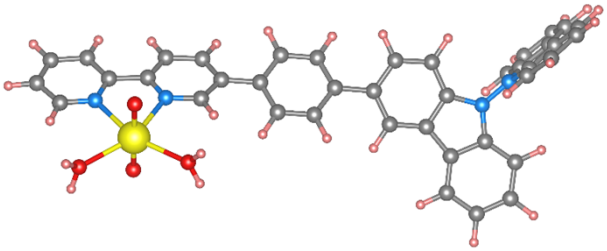

Fig. S10. The adsorption model of $[U(VI)O_2(H_2O)_2]$@Cz-Bpy.

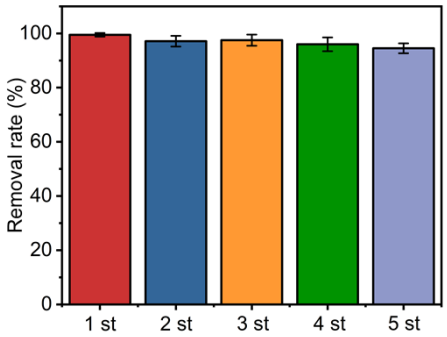

Fig. S11. Recycling U(VI) separation on Cz-Bpy (C_0 = 50 mg/L, m/V = 0.2 g/L, and T = 293 K). The error bars in the figure represent the standard deviations from triplicate tests.

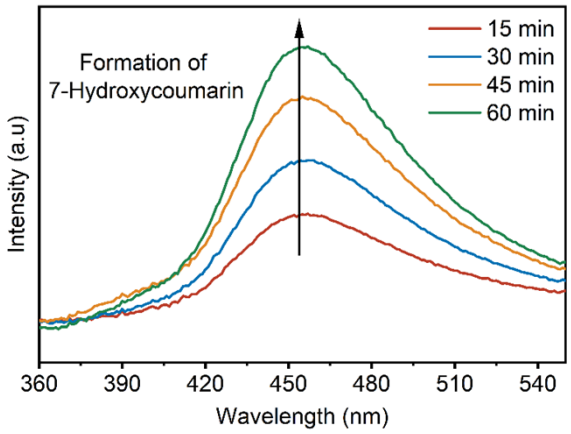

Fig. S12. The conversion of coumarin into 7-hydroxycoumarin by using Cz-Bpy as photocatalyst.

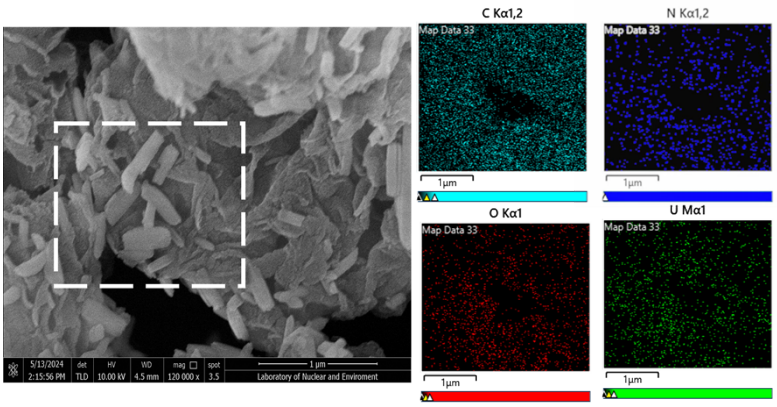

Fig. S13 The SEM and EDS mapping images of Cz-Bpy after photoreaction.

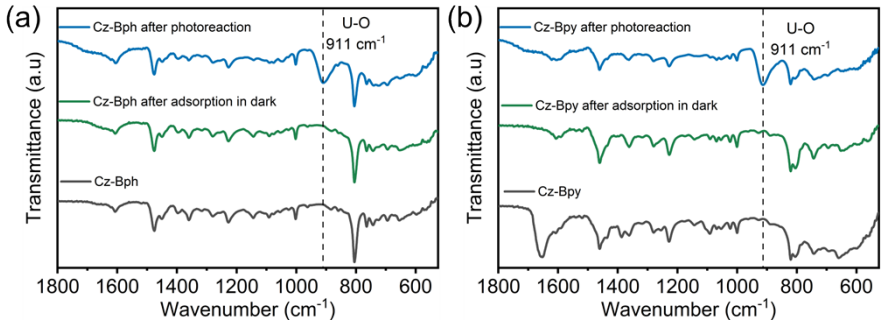

Fig. S14. The FT-IR spectra of Cz-Bph adsorption in the dark condition and photoreaction.

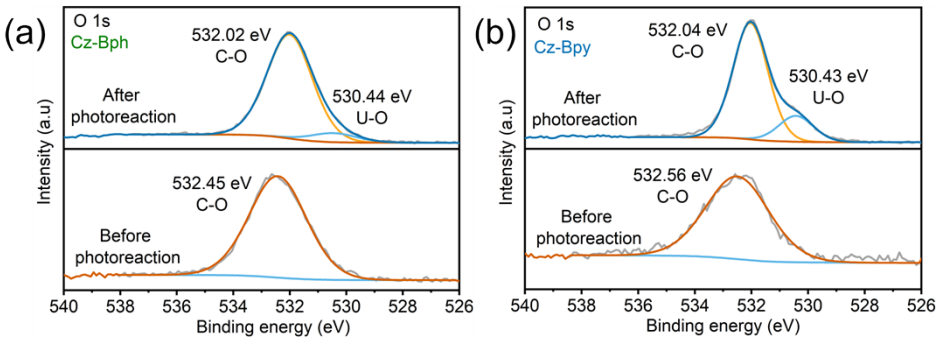

Fig. S15. XPS O 1s spectra of (a) Cz-Bph and (b) Cz-Bpy before and after photoreaction.

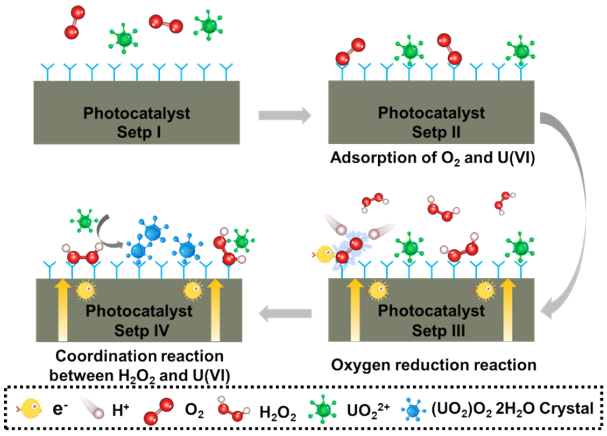

Fig. S16. The corresponding photocatalytic U(VI) separation mechanisms. Step I and Step II, the adsorption of O_2. Step III, the O_2 reduction reaction (ORR) induced by photoelectrons to form H_2O_2. Step IV, the formation of $(UO_2)O_2 \cdot 2H_2O$ induced by the coordination reaction between U(VI) and H_2O_2. The reaction formula is:

$$UO_2^{2+} + H_2O_2 + 2H_20 \rightarrow UO_2(O_2) \bullet 2H_2O + 2H^+ \quad (1)^{13,14}$$

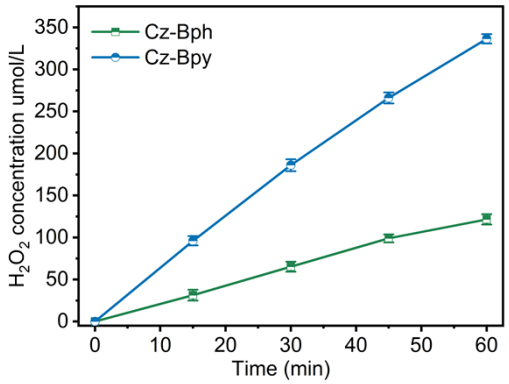

Fig. S17. Time course of photocatalytic H_2O_2 production by Cz-Bph and Cz-Bpy. The error bars in the figure represent the standard deviations from triplicate tests.

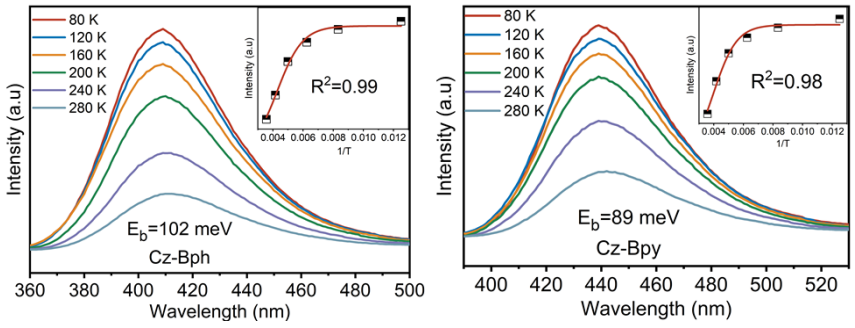

Fig. S18. The TD-PL spectra of Cz-Bph and Cz-Bpy.

Table S1 Comparison of various catalysts for photocatalytic removal of U(VI).

Catalysts	C(U(VI)) (mg/L)	m/V (g/L)	Ligh sources	R (μmol/(g.h))	Ref.
Cz-Bpy	**50**	**0.2**	**Xe lamp**	**404**	**This work**
S-doped g-C_3N_4	28.6	0.5	Xe lamp	98	[10]
$LaFeO_3$/g-C_3N_4	23.8	0.2	Xe lamp	192	[15]
g-C_3N_4/TiO_2	20	0.5	Xe lamp	28	[16]
MoS_2/P-g-C_3N_4	50	1	Xe lamp	210	[17]
CeO_{2-X}/ g-C_3N_4	23.8	0.5	Xe lamp	37	[18]
C_3N_5/GO	10	0.5	Xe lamp	78	[19]
CN550	200	1	Xe lamp	97	[20]
CNNS@CdS	50	1	Xe lamp	96	[21]
UiO-66-NH_2	110	0.2	Xe lamp	64	[22]
Gd/CdS-$PW_{12}AO$	50	4	Xe lamp	52	[23]
graphene aerogel	95.2	0.4	Xe lamp	291	[24]
Br-C_3N_4	40	0.2	Xe lamp	504	[25]
g-C_3N_4/GO	60	0.1	Xe lamp	569	[26]

Table S2. The species and contents of mine wastewater were given by Uranium Industry Co., Ltd in China.

U (mg/L)	CO_3^{2-} (g/L)	Ca^{2+} (mg/L)	Mg^{2+} (mg/L)	SO_4^{2-} (mg/L)	Cl^- (g/L)
61.44	1.13	201	152	1870	13.16

References

1 Y. Yang, L. Li, R.-B. Lin, Y. Ye, Z. Yao, L. Yang, F. Xiang, S. Chen, Z. Zhang, S. Xiang and B. Chen, *Nat. Chem.*, 2021, **13**, 933–939.

2 R. Cheng, R. He, R. Li and W. Zhu, *J. Radioanal. Nucl. Chem.*, 2024, **333**, 1831–1840.

3 F. Aydin, E. Yilmaz, E. Ölmez and M. Soylak, *Talanta*, 2020, **207**, 120295.

4 N. Jalbani and M. Soylak, *J. Radioanal. Nucl. Chem.*, 2014, **301**, 263–268.
5 F. Shah, M. Soylak, T. G. Kazi and H. I. Afridi, *J. Radioanal. Nucl. Chem.*, 2013, **296**, 1239–1245.
6 S. Grimme, J. Antony, S. Ehrlich and H. Krieg, *J. Chem. Phys.*, 2010, **132**, 154104.
7 V. Barone and M. Cossi, *J. Phys. Chem. A*, 1998, **102**, 1995–2001.
8 T. Lu and F. Chen, *J. Comput. Chem.*, 2012, **33**, 580–592.
9 Z. Liu, T. Lu and Q. Chen, *Carbon*, 2020, **165**, 461–467.
10 P. Liang, L. Yuan, K. Du, L. Wang, Z. Li, H. Deng, X. Wang, S.-Z. Luo and W. Shi, *Chem. Eng. J.*, 2021, **420**, 129831.
11 Z. Li, Z. Zhang, Z. Dong, F. Yu, M. Ma, Y. Wang, Y. Wang, Y. Liu, J. Liu, X. Cao and Y. Liu, *Sep. Purif. Technol.*, 2022, **283**, 120195.
12 J. Chang, Q. Li, J. Shi, M. Zhang, L. Zhang, S. Li, Y. Chen, S. Li and Y. Lan, *Angew. Chem. Int. Ed.*, 2023, **62**, e202218868.
13 Y. Hu, D. Tang, Z. Shen, L. Yao, G. Zhao and X. Wang, *Appl. Catal. B*, 2023, **322**, 122092.
14 Z. Li, Z. Zhang, X. Zhu, C. Meng, Z. Dong, S. Xiao, Y. Wang, Y. Wang, X. Cao and Y. Liu, *Appl. Catal. B*, 2023, **332**, 122751.
15 X. Li, J. Wang, F. Xue, Y. Wu, H. Xu, T. Yi and Q. Li, *Angew. Chem. Int. Ed.*, 2021, **60**, 2534–2540.
16 X.-H. Jiang, Q.-J. Xing, X.-B. Luo, F. Li, J.-P. Zou, S.-S. Liu, X. Li and X.-K. Wang, *Appl. Catal. B*, 2018, **228**, 29–38.
17 Z. Li, Z. Zhang, Z. Dong, Y. Wu, J. Liu, Z. Cheng, Y. Liu, Y. Wang, Z. Zheng, X. Cao, Y. Wang and Y. Liu, *J. Solid State Chem.*, 2021, **302**, 122305.
18 S. Li, D. Pan, Z. Cui, Y. Xu, H. Shang, W. Hua, F. Wu and W. Wu, *Sep. Purif. Technol.*, 2022, **301**, 121966.
19 Q. Meng, X. Yang, L. Wu, T. Chen, Y. Li, R. He, W. Zhu, L. Zhu and T. Duan, *J. Hazard. Mater.*, 2022, **422**, 126912.
20 S. Liu, Z. Wang, Y. Lu, H. Li, X. Chen, G. Wei, T. Wu, D.-J. Maguire, G. Ye and J. Chen, *Appl. Catal. B*, 2021, **282**, 119523.
21 F. Wang, Y. Liao, T. Li and L. Xia, *Sep. Purif. Technol.*, 2022, **299**, 121707.
22 N. Zhao, K. Zhang, Y. Lu, S. Liu, Z. Wang and X. Wang, *J. Water Process. Eng.*, 2024, **67**, 106210.
23 Y. Liu, D. Cui, T. Zhang, X. Yang, C. Wang and F. Li, *Chem. Eng. J.*, 2024, **497**, 154416.
24 Z. Wang, H. Liu, Z. Lei, L. Huang, T. Wu, S. Liu, G. Ye, Y. Lu and X. Wang, *Chem. Eng. J.*, 2020, **402**, 126256.
25 J. Xue, B. Wang, Z. Li, Z. Xie and Z. Le, *Res. Chem. Intermed.*, 2022, **48**, 49–65.
26 T. Chen, J. Zhang, H. Ge, M. Li, Y. Li, B. Liu, T. Duan, R. He and W. Zhu, *J. Hazard. Mater.*, 2020, **384**, 121383.